Xenotransplantation 2013: 20: 165–176
Printed in Singapore. All rights reserved
doi: 10.1111/xen.12033

© 2013 John Wiley & Sons A/S

Original Article

Human adipose-derived mesenchymal stem cells can survive and integrate into the adult rat eye following xenotransplantation

Haddad-Mashadrizeh A, Bahrami AR, Matin MM, Edalatmanesh MA, Zomorodipour A, Gardaneh M, Farshchian M, Momeni-Moghaddam M. Human adipose-derived mesenchymal stem cells can survive and integrate into the adult rat eye following xenotransplantation. Xenotransplantation 2013: 20: 165–176.
© 2013 John Wiley & Sons A/S.

Abstract: Background: Novel threads of discovery provide the basis for optimism for the development of a stem-cell-based strategy for the treatment of retinal blindness. Accordingly, achievement to suitable cell source with potential-to-long-term survival and appropriate differentiation can be an effective step in this direction.
Methods: After derivation of human adipose-derived mesenchymal stem cells (HAD-MSCs), they were stably transfected with a vector containing Turbo-green fluorescent protein (GFP) and JRed to be able to trace them after transplantation. Labeled HAD-MSCs were transplanted into the intact adult rat eye and their survival, integration, and migration during 6 months post-transplantation were assessed.
Results: The transplanted cells were traceable in the rat vitreous humor (VH) up until 90 days after transplantation, with gradual reduction in numbers, their adhesion and expansion capacity after recovery. These cells were also integrated into the ocular tissues. Nonetheless, some of the implanted cells succeeded to cross the blood–retina barrier (BRB) and accumulate in the spleen with time.
Conclusions: The survival of the HAD-MSCs for a period of 90 days in VH and even longer period of up to 6 months in other eye tissues makes them a promising source to be considered in regenerative medicine of eye diseases. However, the potency of crossing the BRB by the implanted cells suggests that use of HAD-MSCs must be handled with extreme caution.

Aliakbar Haddad-Mashadrizeh,[1,2] Ahmad R. Bahrami,[1,2] Maryam M. Matin,[1,2] Mohammad A. Edalatmanesh,[3] Alireza Zomorodipour,[4] Mossa Gardaneh,[4] Moein Farshchian[1,2] and Madjid Momeni-Moghaddam[1,2]

[1]Cell and Molecular Biotechnology Research Group, Institute of Biotechnology, Ferdowsi University of Mashhad, Mashhad, [2]Department of Biology, Faculty of Science, Ferdowsi University of Mashhad, Mashhad, [3]Department of Physiology, Science & Research Branch, Islamic Azad University, Fars, [4]National Institute for Genetic Engineering and Biotechnology, Tehran, Iran

Key words: blood–retina barrier – cell integration – cell migration – cell survival – stem-cell therapy – Xenotransplantation

Address reprint requests to Ahmad R. Bahrami, Cell and Molecular Biotechnology Research Group, Institute of Biotechnology, Ferdowsi University of Mashhad, Mashhad, Iran (E-mail: ar-bahrami@um.ac.ir)

Received 28 November 2012;
Accepted 18 March 2013

Introduction

Retinal blinding disorders that are caused by retinal injury, cell death, or cell dysfunction are the predominant causes of human blindness worldwide [1–5]. These disorders together have a prevalence of 1 in 2000 and represent a significant impact on the quality of life as well as the possibility to attain personal achievements [3]. They are rather difficult to treat [2]. Nonetheless, several avenues of research are being pursued to deal with them, including replacement therapies, cell therapy, and pharmacological treatments [1,3,5–9]. Among these approaches, cell-based therapy has been envisaged to restore vision in the patients by repopulating the damaged retina and/or by rescuing retinal neurons from further degeneration [5,6,10]. In this regard, years ago the first report of mammalian retinal transplantation [11] was released in which the use of immature cells and tissues, for retinal replacement, and to some extent the functional recovery were reported [5,12]. However, ethical and logistical hurdles surrounding the cell and immature tissue transplantation procurement highlight the need to identify an alternative cell source. Over the past few years, identification and characterization of stem cells have opened new avenues in cell-

replacement therapy for blindness disorders [6]. On the other hand, the presence of stem cells, including retinal [6] and limbal [7,13] stem cells, in different positions of the eye opens possibilities of regeneration by mobilizing endogenous stem cells to respond to degenerative eye disorders [6]. Accordingly, novel threads of discovery provide the basis for optimism for the development of a stem-cell-based strategy for treatment of the retinal blindness [1,5,7,10]. Embryonic, adult, and induced pluripotent stem (iPS) cell transplantation has been performed into the eye for the treatment of retinal disorders [5,6]. Along with progress in stem-cell-based therapies, a second approach of replacing the impaired genes of the tissue is being practiced in facing the blindness [3,8,9,14]. Despite the reports on potential of embryonic stem (ES) cells in regenerative medicine and blindness treatment [15,16], it suffers seriously from immunogenic and ethical concerns [5]. Moreover, the potential risk of teratogenicity of these cells and also iPS cells [5] led to consider application of adult stem cells as a more suitable cell source in clinical level [17]. Accordingly, adipose-derived mesenchymal stem cells (AD-MSCs) propounded as a novel and ideal source of adult stem cells in regenerative medicine [17–21]. Shortage of access to the stem cells from own sources in one hand and immunerejection of the implanted cells from different sources on the other hand have imposed limitations to progress of the stem cell technology. However to this end, MSCs are generally believed to enjoy cellular and molecular properties to modulate tissue immunological responses [19,21,22], which seems tempting to evaluate the MSC compatibility in even more extreme conditions of xenoplantation. This would add to their value to be applied, from different sources (allograft), in human injuries and further address the long-standing debate of possibility of making human tissues in model animals if experimental evidences are provided and appropriate conditions are introduced. This study sought to take a beginning step by transplantation of human AD-MSCs into the rat eye and test their confinement, maintenance, and integration in the xenogenic conditions.

Materials and methods

Human AD-MSCs handling and transduction

We conducted the study with discarded adipose, by consent of donor, provided kindly by Prof. Sanjar Mousavi, Razavi Haspital, Mashhad, Iran. The tissue had been obtained from a healthy obese woman with age of 44 yr, who underwent esthetic liposuction. Only one session of sampling was performed, and the material was immediately transferred to the clean hood for cell extraction and detached by collagenase digestion and differential centrifugation [23]. Characterization of human adipose-derived mesenchymal stem cells (HAD-MSCs) was performed before and after lentiviral transduction by treating with mesenchymal lineage-specific medium. For osteogenic induction, the cultures were treated with 50 μg/ml ascorbate-2 phosphate, 100 nM dexamethasone (Sigma, Munich, Germany), and 10 mM β-glycerophosphate (Sigma) for a period of 4 weeks and stained with 0.1% (w/v) Alizarin Red solution. For induction of adipogenesis, the cells were treated with 50 μg/ml ascorbate-2-phosphate, 100 nM dexamethasone (Sigma), and 50 μg/ml indomethacin (Sigma) for 3 weeks and stained with 0.5% (w/v) Oil red O (Sigma). The HAD-MSCs were transduced lentivirally to express both green fluorescent protein (Turbo-GFP) and red fluorescent protein (JRed). Briefly, recombinant VSV-G pseudotype lentiviral vector was produced by calcium phosphate cotransfection of HEK293T cells in 10-cm dishes [24]. For this, psPAX2 (21 μg), pMD.2G (10.5 μg) (both from Trono Lab), and pLEX-JRED/Turbo-GFP (21 μg) (Open Biosystems; Fisher Scientific, Pittsburgh, PA, USA) vectors were mixed in Ca3(PO4) 2 solution. After 16 h, the mix was replaced with fresh DMEM, containing 10% FBS. The supernatants were harvested in 24, 48, and 72 h time points and centrifuged 5 min at 500 g (4 °C) to pellet the detached cells, and their debris was filtered through a 0.45-μm filter. Fresh recombinant virus stocks were generated for each experimental use. Titration of the viral particles was determined by performing a p24 ELISA kit (DIA.PRO, Milano, Italy) to detect the HIV-p24 core protein of the vector. Then, undifferentiated HAD-MSCs at passage 3 were plated at a density of 3×10^6 cells per flask (T75), left to settle for 2 days, and subjected to transduction. The efficiency of transduction was assessed by monitoring the GFP gene expression using fluorescent microscopy. The cultures were then subjected to puromycin-containing medium (1 μg/ml puromycin; Sigma) 72 h after transduction. The labeled cells were used for transplantation into the rat organs in following experiments.

Experimental animal and cell transplantation

In all stages of this study, we used 2-month-old Wistar rats with average weight of 250 g. Animals were kept in normal day–night cycle (12/12), stan-

dard temperature (25 ± 2 °C), and humidity conditions and also fed by laboratory chow and tap water. All experiments were carried out in accordance with the Guidelines of the Animal Care of Ferdowsi University of Mashhad and were approved by the Animal Ethics Committee of our university. For transplantation, animals were anesthetized using a mixture of ketamine (30 mg/kg) and xylazine hydrochloride (4 mg/kg). Animals received intraocular GFP-labeled HAD-MSCs, injected through the dorsolateral aspect; the exact way of injection was through sclera in pars plana point which was aimed to deliver the cells into the vitreous cavity of the eye using a 30-gauge insulin syringe. In the test group (n = 32), 10 µl of the transformed HAD-MSCs was resuspended in phosphate-buffered saline (PBS) (20 000 cells/µl) and slowly injected into the vitreous chamber of the animals. The same volume of PBS was injected into the vehicle rats (n = 32) in the same coordinates. Moreover, a number of animals (n = 24) were subjected to liver injection of the labeled HAD-MSCs as control groups to evaluate the potency of blood–retina barrier (BRB) in prevention of the cell migration. Following surgery, 50 000 units of penicillin/kg body weight were injected intraperitoneally. After recovery, the animals were returned to their cages and assessed at different time points up to 6 month.

Isolation, expansion, and quantification of the implanted cells

At different time points of 2, 24, 96, 168 h and 15, 45, 90, and 180 days post-transplantation, four rats in each group were re-anesthetized as described above and sacrificed by cardiac perfusion. The left ventricle was cannulated, an incision was made in the right atrium, and they were perfused with 4% paraformaldehyde in PBS, containing 100 mM $CaCl_2$ and 1 M $MgCl_2$ with pH 7.4, until the outflow runs clear. The eyes were dissected out and washed by disinfectant solutions (40 and 10% v/v Savlon, 70% ethanol, and PBS) containing antibiotics (100 units/ml of penicillin and 100 g/ml of streptomycin). The eyes were then located in the 12-well cell culture plates (Nunc, Thermo Scientific, UK), containing Dulbecco's modified Eagle's medium with high glucose (DMEM-HG) (Gibco, Roskilde, Denmark), supplemented with 10% (v/v) FBS (fetal bovine serum; Gibco), and were fragmented to release the implanted cells from vitreous humor (VH). Ocular tissues were removed from the culture plate and post-fixed immediately in 4% paraformaldehyde for at least 24 h until performance of histological analyses. The cultures were maintained at 37 °C and 10% CO_2. Moreover, ImageJ software was used to quantify the number of recycled cells, as an indicator of their survival rate in the implanted organ.

Histological analysis and quantification of the implanted cells

The examined ocular tissues as described above, as well as the spleens, as known residing organ for the migrated cells in cell transplantation [25–27] of the same rats were harvested and embedded in paraffin (Merck, Berlin, Germany). A rotary microtome (Leitz, Sydney, Australia) was used to prepare 5-µm horizontal sections of the eyes and spleens. Slides were stained by hematoxylin/eosin (HE) and DAPI nucleic acid stain and examined under a light and fluorescent microscope (Olympus AH3-RFCA, Tokyo, Japan). Moreover, ImageJ software was used to quantify the number of the integrated cells in the ocular tissues, as an indicator of their survival rate in the implanted organ. All labeled cells were monitored in 10 microscopic slides, representing an individual eye, and four eyes were examined each time.

DNA extraction and PCR analysis

Total genomic DNA (gDNA) was extracted from rat spleens, using AccuPrep Genomic DNA Extraction Kit (Bioneer, Daejeon, South Korea) according to the manufacturer's protocol. The isolated gDNA was directly used for detection of presence of the Turbo-GFP gene in the genome by standard PCR analysis method. The forward and reverse primers used for amplification were as follows: 5′-GATGAAGAGCACCAAAGGC-3′ and 5′-GTAGCTGAAGCTCACGTGC-3′, respectively. The thermal cycling condition was started with one cycle at 95 °C for 5 min, followed by 40 cycles at 94 °C for 30 s, 59 °C for 30 s, 72 °C for 30 s, and extra cycle at 72 °C for final extension for 5 min. For negative controls, gDNAs from the vehicle and control rats were used. For positive controls, gDNAs from the positively transduced HAD-MSCs were used. PCR product, a fragment of turbo-GFP with 220 base pair (bp) length, was separated on 2% agarose gel and visualized and photographed under the UV light after staining with ethidium bromide.

Quantitative real-time PCR analysis

The copy number of GFP marker gene, as an indicator of cell migration from the implanted sites (eye and liver), was quantified with absolute

real-time PCR (Bio-Rad CFX-96 thermocycler) using the gDNAs from spleens as template. A 7-fold serial dilution series of pLEX-JRed/Turbo-GFP, ranging from 8.5×10^2 to 8.5×10^8 copies/μl, was used to construct the standard curve. The mass concentration of the GFP carrying vector, pLEX-JRed/Turbo-GFP, was measured using a NanoDrop (Thermo Scientific nanodrop 2000c, Thermo Scientific, Wilmington, DE, USA) and converted to the copy concentration using the following equation: DNA (copy) = 6.02×10^{23} (copies/mol)/DNA length (bp) × 660 (g/mol/bp) [28]. Each standard dilution was prepared in duplicate for further analysis. The threshold cycle (CT) values were plotted against the logarithm of their initial template copy concentrations. Each standard curve was generated by a linear regression of the plotted points. From the slope of each curve, the PCR amplification efficiency (E) was calculated according to the following equation: $E = 10^{-1/\text{slope}} - 1$. Real-time PCR was performed in a Bio-Rad CFX-96 thermocycler. All real-time PCR runs were performed in technical duplicates, and each reaction mixture was prepared using the SYBRGreen I PCR Master Mix (Life Technologies, Carlsbad, CA, USA) in a total volume of 20 μl: 10 μl Master Mix, 3 μl of each sample gDNA (1 ng/μl), 0.5 μl of each primer (10 pmol/μl), and 6.5 μl DNase-free water, using absolute quantitative ΔCt method [29]. The thermal cycling conditions were as follows: initial denaturation for 10 min at 95 °C followed by 40 cycles at 95 °C for 40 s, 59 °C for 30 s, and 72 °C for 30 s.

RNA extraction and quantitative real-time RT-PCR analysis

Total RNA was isolated from the dissected eyes at 3 months of post-transplantation, using Trizol reagent (Bioneer) according to the manufacturer's protocol. The RNA samples were treated with RNase-free DNase I (Fermentas, Leon-Rot, Germany) to remove contaminating genomic DNA. Concentration and purity of the total RNA were determined using the NanoDrop (Thermo scientific nanodrop 2000c). The quality of RNA was analyzed by electrophoresis on 1% agarose gel. Approximately 2 μg of total RNA was reverse transcribed using Moloney Murine Leukemia Virus Reverse Transcriptase (MMLV-RT; Fermentas), primed with Oligo dT, at 42 °C for 1 h in a final volume of 20 μl. The expression of some critical differentiating factors was quantified by quantitative real-time PCR (CFX-96; Bio-Rad, Hercules, CA, USA). The reaction tubes included the cDNA, as templates, plus a pair of human specific primers, and SYBRGreen I PCR Master Mix (Applied Biosystems). The cycling conditions were as follows: 95 °C for 10 min; 40 cycles of 95 °C for 15 s; then 58 °C for 30 s, 72 °C for 30 s) in a 20-μl reaction volume. All results were normalized relative to the expression of human glyceraldehyde-3-phosphate dehydrogenase (GAPDH) and fold change expression of desired tissue was calculated by delta-delta Ct method. Human specific primers for the genes of interest were selected based on the previously published reports including the following: human PAX6 forward 5′-CCGTGTGCCT CAACCGTA-3′, reverse 5′-CACGGTTTACTGG GTCTGG-3′ [30], human OTX2 forward 5′-GAG AGCATTGGTAGGCTCC-3′, reverse 5′-TCTCC ACAGTCCCATACTCG-3′ [31], human CRX forward 5′-TCAGATCTTGTAGAGGACGCAG-3′, reverse 5′-CTCTCCCTGTGGAGGAAAG-3′ [32], and human GAPDH forward 5′-GACCACTTT GTCAAGCTCATTTCC-3′, reverse 5′-GTGAG GGTCTCTCTCTTCCTCTTGT-3′ [33].

Statistical analysis

One-way analysis of variance (ANOVA) was used to analyze the isolation, survival, and migration of the implanted HAD-MSC over time, and paired sample t-test was used to determine the effect of BRB on cell migration. Analysis of variance was performed by a Tukey post hoc test. Statistical significance was considered at $P < 0.05$ and $P < 0.001$. All data were expressed as mean ± standard deviation and carried out in triplicates with SPSS 16.0 (SPSS Inc., Chicago, IL, USA).

Results

HAD-MSC Characterization and genetic modification

The plasticity of the isolated cells was assessed 3 weeks after lineage induction in the normal-and viral-transduced cells. Adipogenic and osteogenic differentiations were demonstrated by the expressions of lipid vacuoles and calcium deposits, respectively (Fig. 1). The cells were also subjected to flow cytometry analysis for expression of the MSC markers and shown to be positive for the antigens of CD44, CD105, and CD90 and negative for CD45 and CD34 markers (data not shown). These results confirmed the mesenchymal nature of the isolated and transduced cells as well as their multipotent potential. Furthermore, 24 h after infection of the cells with viral particles carrying the genes for GFP and JRed, isolated green and red cells were observed and they began to expand when subjected to puromycin-containing medium (Fig. 2).

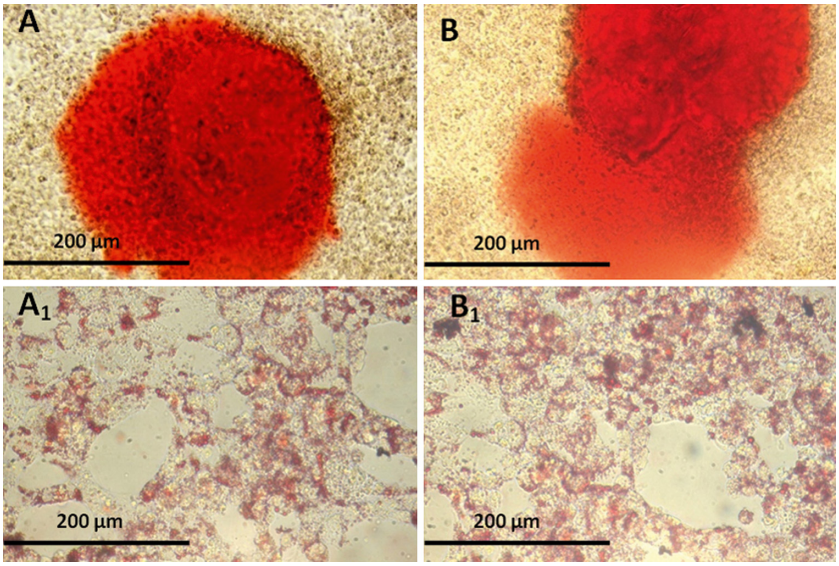

Fig. 1. Osteogenesis and adipogenesis in human adipose-derived mesenchymal stem cells after their exposure to the corresponding conditions and staining with Alizarin Red (upper panel) and Oil red O (lower panel), respectively. (A, and A1) the differentiated cells before the viral transduction, and (B, and B1) the differentiated cells after the viral transduction.

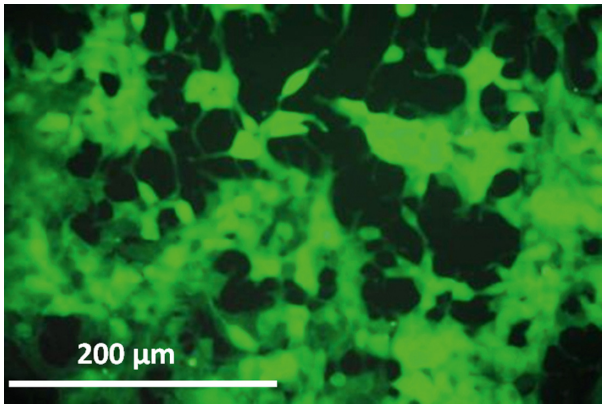

Fig. 2. Expression of the green fluorescent protein transgene in the lentivirally transduced human adipose-derived mesenchymal stem cell, 21 days after exposure to the selection (puromycin containing) medium.

Survival and integration of the implanted HAD-MSCs in rat ocular tissues

As shown in Table 1, the expression of reporter genes, as an indicator of cell survival, was persistent in the examined tissues during 6 months period of experiment. The implanted cells were shown to survive and integrate well into the host ocular tissues (Fig. 3).

Spatial and temporal change of the transplanted cells in the ocular tissue

The implanted cells were shown to migrate well through the host ocular tissues (Fig. 4). As shown in this figure, the transplanted cells were identified in various segments of the eye including VH (Fig. 4A), retina (Fig. 4A), and choroid at each time of examination. The implanted cells could be seen proximate to the vessels in the choroid layer.

Integration and differentiation of the transplanted HAD-MSCs

The transplanted cells tended to penetrate into the host tissue by adopting a spindle-like shape with time. These data were further confirmed by measurement of gene expression at mRNA level for three genes expressed in eye progenitor cells. As shown in Fig. 5, the expression of CRX and PAX6 genes was increased significantly at 90 days post-transplantation.

Isolation and recovery of the implanted HAD-MSCs from VHs

To test the possibility of recovery of the cells and their further characterization, the implanted VHs were subjected to selective cell culture. Upon the culture in DMEM-HG containing antibiotics, the labeled cells were successfully recovered (Fig. 6). Their density, however, tended to decrease by the time (Fig. 7). Among the isolated cells, only those recovered from VHs corresponding to 2, 24, 96, and 168 h after implantation maintained their adhesion capacity after recovery. Nonetheless, only those derived from the periods of 2 and 24 h continued to keep their expansion capacity.

Migration of the implanted cells from the blood–retina barrier

PCR technique on the GFP marker gene was employed to evaluate the ability of BRB in confining the cells within the eye and prevention of them from migrating to non-targeted organs. This analysis proved positive in gDNA extracted

Table 1. Qualitative assessment of survival and behavior of the human adipose-derived mesenchymal stem cells in the ocular tissues of adult rat based on detection of the fluorescent cells, during 6 months post-transplantation

Time	Hours							Days						
Character	2	24	96	168	15	45	90	180						
Green fluorescent protein-expression	+	+	+	+	+	+	+	+	+	+	+	+	+	+
JRed-expression	+	+	+	+	+	+	+	+	+	+	+	+	+	+
Isolation from eye	+	+	+	+	+	+	+	+	+	+	+	+	−	−
Attachment to flask	+	+	+	+	+	+	+	+	+	+	+	+	−	−
In vitro Expansion	+	+	+	+	+	+	+	+	+	+	+	+	−	−
Tissue Integration	−	−	−	−	−	−	−	−	−	−	−	−	−	−
Migration from blood–retina barrier	−	−	−	−	−	−	−	−	+	+	+	+	+	+

The positive and negative signs just indicate the general trend of presence and absence of the character without carrying scoring significance. In limited cases of groups, however, the observations do not seem consistent for all members of the group. This could be caused by silencing of the fluorescent gene in the labeled cells or technical problem in detection of the cells. As shown in this table, expressions of the reporter genes were detectable in each experiment up to 180 days. Although the cells are shown to be integrated into the host tissues, they manage to migrate to other organs as well. The possibility to re-isolate the implanted cells and grow them in culture and also their ability to attach to the plates and expand are reported here. Integration to ocular tissues was observed from 15 days after transplantation. Transplanted cells succeeded to cross the blood–retina barrier from 96 h after implantation. The experiments were performed at eight different, shown, time points. For each time point, four rats were included and their individual results are shown in separate columns. However, these observations were not consistent in all members of the group at some time points.

from spleens, even 6 months after implantation (Fig. 8). Moreover, we have also tracked HAD-MSCs in other organs, including muscle, lung, and skin, 3 months after transplantation (Fig. 9).

Quantitative measurement of the HAD-MSC migration from the blood–retina barrier

To compare the capacity of the BRB in prevention of cell migration, the copy number of the GFP marker gene, as an indicator of quantitative number of the implanted cells, was assessed in the spleens of two groups, which had received the labeled cells in their eye with blood barrier (WB), and liver, without blood barrier (WOB) by absolute real-time PCR procedure. As shown in Fig. 10, the labeled cells were tracked in the spleens of both groups with significant differences at different time points. Accordingly, at the first period of the examination, 96 h up to 15 days, the numbers of the labeled cells were significantly higher in the spleens of the WOB group compared with that of the WB group. This number tended to decrease by time in WOB group up to 180 days. On the other hand, the number of the labeled cells increased significantly at 90 days after transplantation in the WB group.

Discussion

The ideal cell population for cell-based therapy of blindness should be amenable to expansion, directed differentiation, correct integration to ocular tissues, free of malignant potential, and immunogenicity [5,7]. Several features of the adipose-derived MSCs make them an excellent candidate for this purpose [22,34,35]. Accordingly, in this study, long-term survival of the labeled human AD-MSCs, with the knowledge that MSCs transduced with viral vectors do not change their biological and other properties [36–38], and also the capacity of the BRB for confinement the migration of these cells were tested. Because the cells were aimed to be delivered into the vitreous cavity, the exact way of injection was through sclera in pars plana point. This would minimize the chance of cell injection to other tissues, such as retina. To avoid potential damages from high volume of injection, we reduced the volume to half from what was reported before [39] where they used 20 µl. Survival and integration of the implanted cells in the recipient eyes for up to 6 months clearly support the idea of hypoimmunogenic property of the donor and host systems. These results are consis-

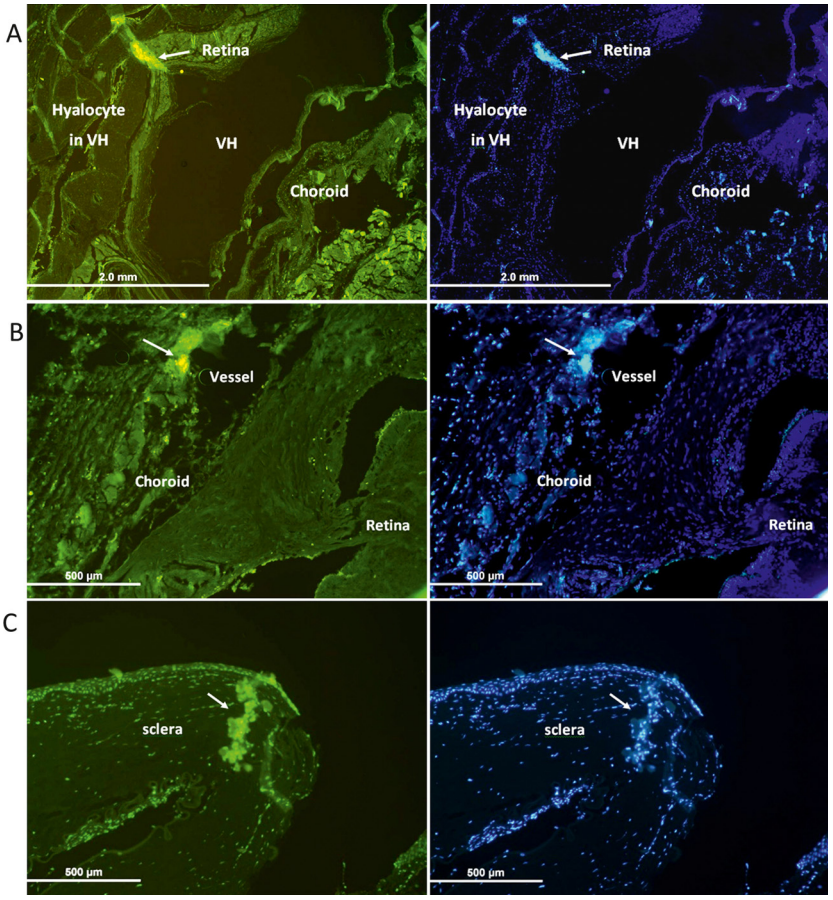

Fig. 3. Micrographs representing integration (pointed by arrows) of the human adipose-derived mesenchymal stem cells into the rat ocular tissues at different time points of 15, 45, and 180 days post-implantation, which correspond to the panels A–C, respectively. The first column represents integration of the cells into ocular tissues expressing green fluorescent protein. The second column represents the DAPI-stained cells to confirm their cellular integrity.

tent with former report, showing the prolonged survival of foreign (allogenic and xenogenic) cells and tissues after transplantation into the anterior chamber of the eye [5,40–42]. However, the number of the recovered human AD-MSCs from the rat VH after transplantation was reduced by the time, as there were no detectable cells 90 days after transplantation in the VH. This could be due to reporter gene silencing [43], homing to the ocular tissues, and migration from BRB. Our results indicate that the implanted cells could be integrated into the ocular tissues from 15 days after implantation (Fig. 3), which is consistent with the homing property of the stem cells [35]. In this regard, several other reports have also demonstrated that different cell types as well as AD-MSCs could be integrated into the ocular tissues, especially retina, when transplanted into the VH [5,41,42,44–46]. Despite the integration (Fig. 3) and the possibility of MSC differentiation to the ocular tissues, including the retina cells in the transplanted VH which was clearly demonstrated by expression analysis of the molecular markers specific for ocular tissues (Fig. 5) by RT-PCR, our experiments missed the chance, in histological level, to track presence of the injected cells in the retina tissue due to technical limitations in our histological examination, as the retina is very delicate tissue and disrupted easily during the section preparation, leaving some debris (Fig. 4A). However, our results clearly show that the reduction in the primary number of the cells over the time is at least partly due to their migration from the VH, by crossing the known blood barrier and reach into the spleen and other organs (Figs 8 and 9). This adds more controversy to the notion that views the eye as an impermeable organ, by the specific morphological architecture of its borders which are surrounded by blood barriers [54–56]. The pass can only be speculated from our data (Fig. 4). In this study, we used presence of vessels as an indication for tracking the choroid and accordingly noticed that the injected cells migrate from the original points of injection toward margins of vessels in the choroid tissue, which is tempting to suggest these vessels as potential way of migration to other ocular tissues, such as sclera, or even other organs, such as spleen. One could think these cells are present in sclera due to efflux from the injection. This is unlikely because these cells can be detected in sclera even

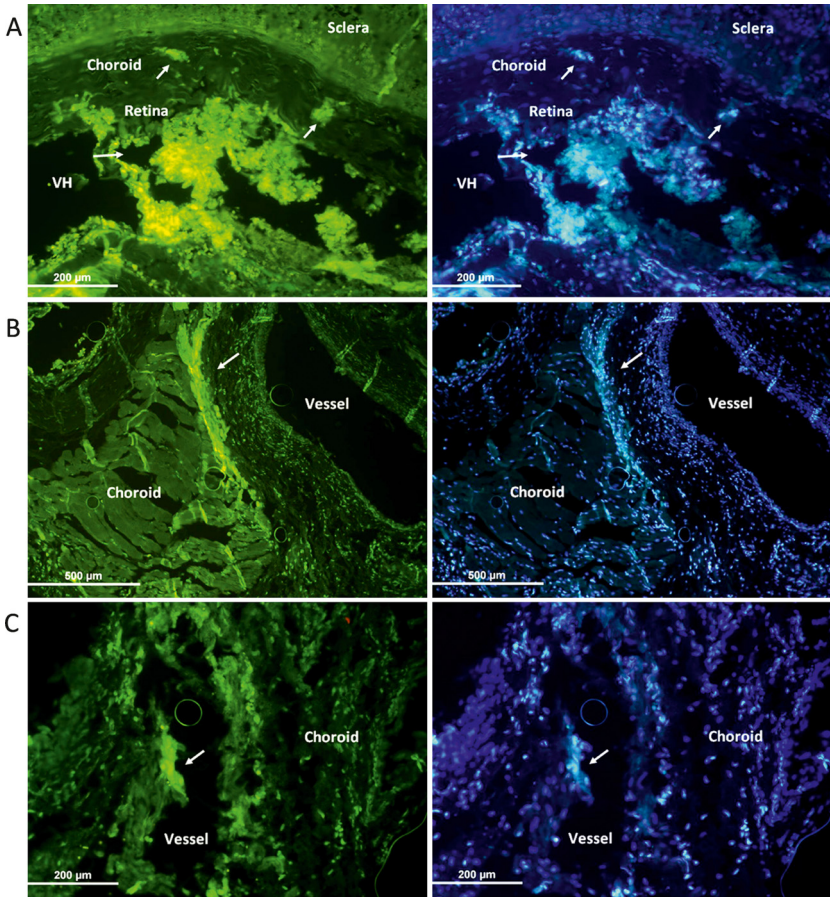

Fig. 4. The spatial and temporal change of the transplanted cells in the ocular tissue 15 days after injection. The cells (pointed by arrows) are settled well in the vitreous humor (panel A) and integrated into the choroid layer (panel B). They reach to the vicinity of the vessels in the choroid (panel C). First and second columns represent fluorescent signals from green fluorescent protein-labeled cells and DAPI staining, respectively.

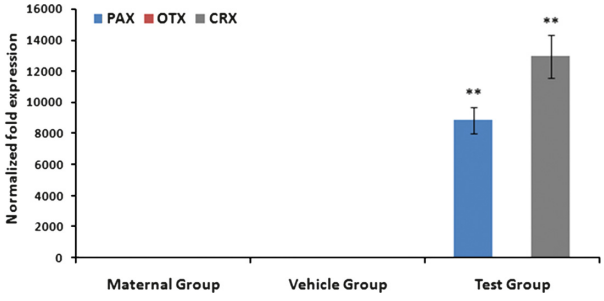

Fig. 5. Expression of mRNAs specific for eye progenitor cells after transplantation of human adipose-derived mesenchymal stem cells into the rat eye. The data represent the averages of three independent measurements of mRNA level for three genes of PAX6, OTX2, and CRX by real-time PCR method. Asterisks and the error bars represent $P \leq 0.001$ and the standard deviation (SD), respectively.

after long period of up to 6 months as seen in Fig. 3C, which support the idea of their gradual release from the VH. To this end, we chose spleen for tracking footprints of the migrated cells. This experiment was performed by looking for GFP-positive cells which was a specific character of the xenogenic implanted cells and proved that these cells had reached and resided in the spleen. The general belief is that upon phagocytosis of a cell by macrophages, it is engulfed by phagosome followed fusion to the lysosome which would lead to whole cell degradation including its DNA content [47–49]. This would leave no room for GFP gene to be carried by macrophages to spleens, and other organs. Meanwhile, tracking the signs of DNA for GFP in spleen is not enough to claim presence of the intact migrated cells and this remained to be tested by other means. We also showed that if the labeled cells are injected into the organ WOB i.e. liver, they would find themselves in spleen and are destroyed very quickly (Fig. 10). The same cells, however, if injected to the VH can be detected for long period of time in the spleen, due, may be, to their gradual escape from the blood barrier. Interestingly, our unpublished data confirmed that HAD-MSCs show very high level of CXCR4. This receptor is considered as main player in cell migration [46]. On the other hand, we could track the implanted cells in the choroid at different time points after injection as indicated in the Figs 3(B) and 4(B,C). It can be speculated that these cells are delivered to the systematic circulation from choroid. It is important to note that, cell migration from the trans-

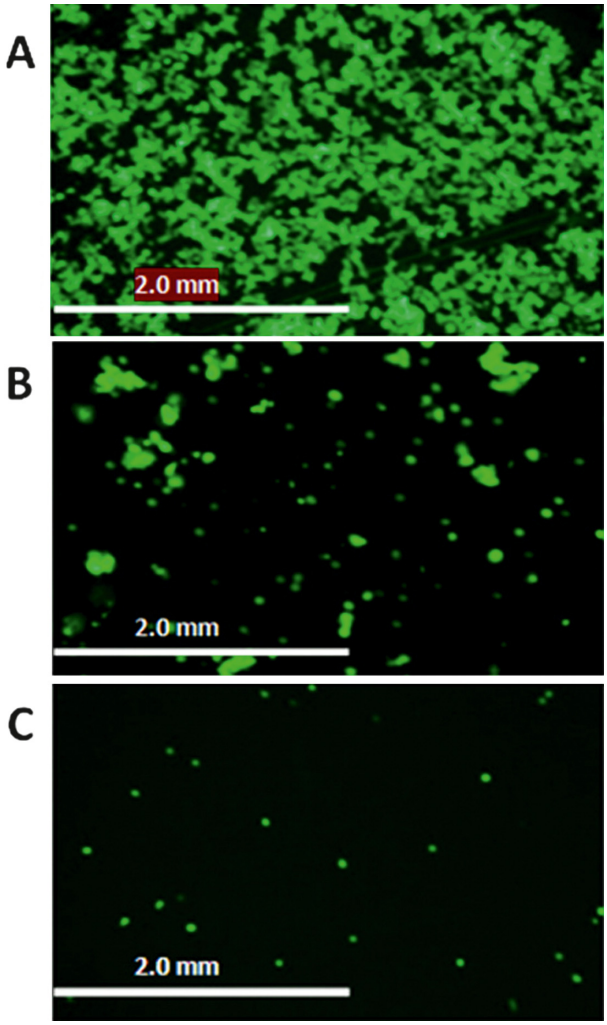

Fig. 6. Isolated human adipose-derived mesenchymal stem cells from vitreous humors at different time courses, including 24 h, 15, and 90 days post-implantation, which correspond to the panels A–C, respectively. The column represents isolated cells expressing green fluorescent protein.

planted site to unwanted organs is one of the main challenges in cell-based therapeutic method [50–53]. Alterations of this barrier contribute to the pathology of a wide number of ocular disorders for leukocyte migration across the BRB [54,56,57]. A large body of evidences demonstrate a clear role for altered expression of cytokines and growth factors which increase BRB permeability with various mechanisms [57,58]. In this regard, it was demonstrated that high concentration of intraocular insulin-like growth factor-I (IGF-I) triggers processes that lead to BRB breakdown. This is thought to happen via IGF-I receptor and vascular endothelial growth factor (VEGF) expression induction [57], as there is a direct correlation between VEGF vitreous levels and BRB permeability [57,59]. On the other hand, there is a significant relationship between VEGF and interleukin-6 (IL-6) levels in VH [60–62]. These results suggest that IL-6 and VEGF may promote the BRB permeability in ocular disorders. It is interesting to note that the potency of various cytokines secretion, such as VEGF, and IL6, from adipose-derived MSCs, specially at the hypoxia condition, has been stimulated [52,63]. This condition is thought to be provided perfectly by eye microenvironment [64,65]. On the other hand, adhesion and expansion capacity of the implanted cells were reduced after recovery from the VH, and they seemed to adopt the spindle shape morphology of the host tissue cells after integration. These alterations might be related to the influence of their new microenvironment in the eye. It is known that alterations in the cell morphology, transcript profiles, marker proteins, and function of cell–cell and cell-matrix adhesion molecules are fully correlated

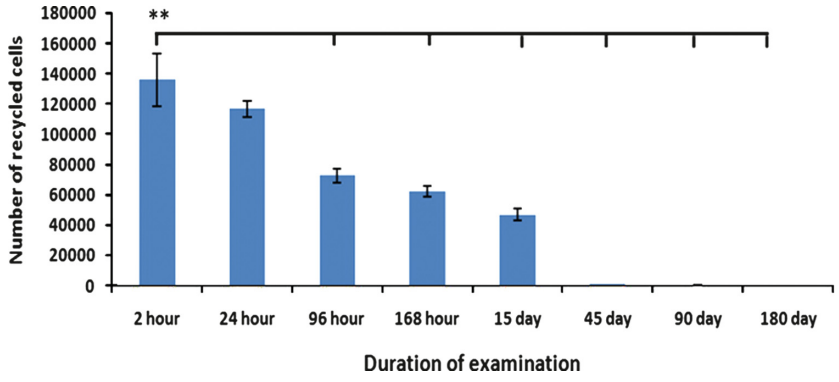

Fig. 7. Quantitative comparison of the isolated human adipose-derived mesenchymal stem cells from rat vitreous humors during 6 months after transplantation, based on average cell counts of the labeled cells. As shown in this Figure, at the beginning times, numbers of the isolated cells were very close to the number of implanted, but they start to decrease by the time. ** represents $P \leq 0.001$. All error bars indicate the standard deviation (SD).

with stem cell differentiation to particular lineage [66–70]. VH is a gelatinous, colorless, and shapeless mix of different substances containing a mass of extracellular matrix, especially hyaluronic acid and collagen fibrils [69], with well-known effects on cellular behaviors including proliferation, migration, and differentiation into the in vitro and in vivo situation [40,41,69]. So, these could be considered as an indication of the influence of the various growth factors or cytokines of the VH [71,72] on alteration of the adhesion and expansion capacity of the implanted HAD-MSCs after their recovery from eye and in vitro culture.

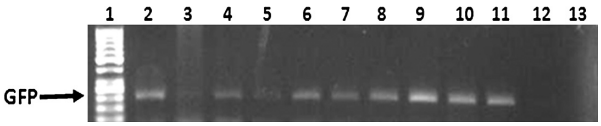

Fig. 8. Presence of green fluorescent protein encoding gene in the rat spleen during 6 months after transplantation, as examined by PCR, representing human adipose-derived mesenchymal stem cells migration from the original transplanted site of the eye. The lanes represent as follows: (1) 50 bp DNA ladder, (2) PCR product on gDNA, as positive control, from the cultured cells in vitro, (3 to 11) PCR products on gDNA extracted from spleens of different rats in the test group from 96 h up to 6 months post-transplantation, including lane 3 (96 h), Lane 4 (168 h), Lanes 5, 6 (15 days), Lanes 7, 8 (45 days), Lanes 9, 10 (90 days), and Lane 11 (180 days) post-transplantation. Lanes 12 and 13 correspond to PCR on spleen gDNA of non-transplanted rats (negative control) and transplanted rats with phosphate-buffered saline (vehicle control), respectively.

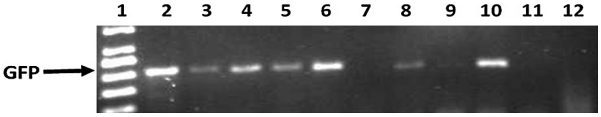

Fig. 9. Human adipose-derived mesenchymal stem cells (HAD-MSCs) mining in different organs, 3 months after transplantation into the rat eyes, based on PCR analysis. Lanes 1 to 2 represent DNA ladder (50 bp; Fermentas) and positive control (gDNA from transduced HAD-MSCs in culture), respectively. Lanes 3 to 5 represent PCR products on gDNA extracted from lung tissues of different rats in the test group. Lanes 6 to 8 represent PCR products on the gDNA extracted from skin tissues of different rats in the test group. Lanes 9 to 10 represent PCR products on the gDNA from muscle tissues of different rats in the test group. Lanes 11 and 12 correspond to PCR products on DNA of non-transplanted rats (negative control) and transplanted rats with phosphate-buffered saline (vehicle control).

Conclusions

Our findings are consistent with former reports about differentiation, integration, and also hypoimmunogenic property of HAD-MSCs, which lead to long-term survival of them not only in the eye, as an immune privilege organ, but also in the spleen which enjoys the excessive immune surveillance. These data would suggest more investigations on the value of the HAD-MSCs as a suitable cell source and differentiation to different tissues in the eye. Nonetheless, tracing footprints of the cells in non-targeted organs is an alarming point to be looked more cautiously before a large-scale clinical trial is performed.

Acknowledgments

This work was financially supported by a grant of Iranian Council of Stem cell Technology (ICST) and performed in Institute of Biotechnology, Ferdowsi University of Mashhad. The authors are grateful to Dr Nasser Mahdavi Shahri, Hassan Tamadonipour, Mohammad Nakhaei, Sohrab Bozarpour, Maryam Sheikh Bahai, and Mahmood Raees-al-Mohaddesin for their technical assistance.

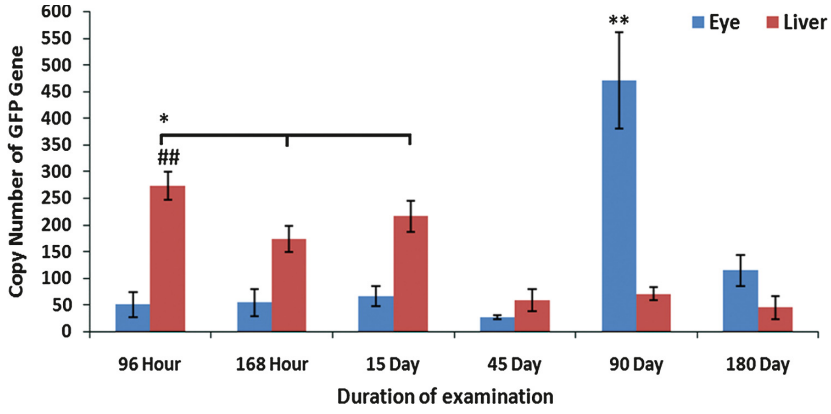

Fig. 10. Quantitative comparison of the human adipose-derived mesenchymal stem cells which resided in the spleen of rats, as a result of migration from the original transplanted sites of the eye and liver, as examined by absolute real-time PCR aiming the green fluorescent protein encoding gene, ($^{\#\#,}$ **P $\leq$ 0.001, *P $\leq$ 0.05). All error bars indicate the standard deviation (SD).

References

1. Bi YY, Feng DF, Pan DC. Stem/progenitor cells: a potential source of retina-specific cells for retinal repair. Neurosci Res 2009; 65: 215–221.
2. Jin ZB, Okamoto S, Mandai M, Takahashi M. Induced pluripotent stem cells for retinal degenerative diseases: a new perspective on the challenges. J Genet 2009; 88: 417–424.
3. Lorenz B, Preising M, Stieger K. Retinal blinding disorders and gene therapy–molecular and clinical aspects. Curr Gene Ther 2010; 10: 350–370.
4. Matthaei M, Zeitz O, Keseru M et al. Progress in the development of vision prostheses. Ophthalmologica 2011; 225: 187–192.
5. Singh MS, Maclaren RE. Stem cells as a therapeutic tool for the blind: biology and future prospects. Proc Biol Sci 2011; 278: 3009–3016.
6. Goureau O, Sahel JA. Retinal stem cells: mechanism of differentiation and therapeutic application. Pathol Biol (Paris) 2006; 54: 64–71.
7. Wallace VA. Stem cells: a source for neuron repair in retinal disease. Can J Ophthalmol 2007; 42: 442–446.
8. Corredor RG, Goldberg JL. Electrical activity enhances neuronal survival and regeneration. J Neural Eng 2009; 6: 055001.
9. Ashtari M, Cyckowski LL, Monroe JF et al. The human visual cortex responds to gene therapy-mediated recovery of retinal function. J Clin Invest 2011; 121: 2160–2168.
10. Bull ND, Martin KR. Using stem cells to mend the retina in ocular disease. Regen Med 2009; 4: 855–864.
11. Tansley K. The development of the rat eye in graft. J Exp Biol 1946; 22: 221–224.
12. Maclaren RE, Pearson RA, Macneil A et al. Retinal repair by transplantation of photoreceptor precursors. Nature 2006; 444: 203–207.
13. Boulton M, Albon J. Stem cells in the eye. Int J Biochem Cell Biol 2004; 36: 643–657.
14. Zhang X, Li GL. Progress in treatment of retinitis pigmentosa by neurotrophic factors. Zhonghua Yan Ke Za Zhi 2009; 45: 855–859.
15. Lamba DA, Karl MO, Ware CB, Reh TA. Efficient generation of retinal progenitor cells from human embryonic stem cells. Proc Natl Acad Sci USA 2006; 103: 12769–12774.
16. Lamba DA, Gust J, Reh TA. Transplantation of human embryonic stem cell-derived photoreceptors restores some visual function in Crx-deficient mice. Cell Stem Cell 2009; 4: 73–79.
17. Strem BM, Hicok KC, Zhu M et al. Multipotential differentiation of adipose tissue-derived stem cells. Keio J Med 2005; 54: 132–141.
18. Zuk PA, Zhu M, Ashjian P et al. Human adipose tissue is a source of multipotent stem cells. Mol Biol Cell 2002; 13: 4279–4295.
19. Rodriguez AM, Elabd C, Amri EZ, Ailhaud G, Dani C. The human adipose tissue is a source of multipotent stem cells. Biochimie 2005; 87: 125–128.
20. Vieira NM, Brandalise V, Zucconi E et al. Human multipotent adipose-derived stem cells restore dystrophin expression of Duchenne skeletal-muscle cells in vitro. Biol Cell 2008; 100: 231–241.
21. Sowa Y, Imura T, Numajiri T, Nishino K, Fushiki S. Adipose-derived stem cells produce factors enhancing peripheral nerve regeneration: influence of age and anatomic site of origin. Stem Cells Dev 2012; 21: 1852–1862.
22. Gimble JM, Katz AJ, Bunnell BA. Adipose-derived stem cells for regenerative medicine. Circ Res 2007; 100: 1249–1260.
23. Gimble J, Guilak F. Adipose-derived adult stem cells: isolation, characterization, and differentiation potential. Cytotherapy 2003; 5: 362–369.
24. Zufferey R, Dull T, Mandel RJ et al. Self-inactivating lentivirus vector for safe and efficient in vivo gene delivery. J Virol 1998; 72: 9873–9880.
25. Gao J, Dennis JE, Muzic RF, Lundberg M, Caplan AI. The dynamic in vivo distribution of bone marrow-derived mesenchymal stem cells after infusion. Cells Tissues Organs 2001; 169: 12–20.
26. Kraitchman DL, Tatsumi M, Gilson WD et al. Dynamic imaging of allogeneic mesenchymal stem cells trafficking to myocardial infarction. Circulation 2005; 112: 1451–1461.
27. Ushiki T, Kizaka-Kondoh S, Ashihara E et al. Noninvasive tracking of donor cell homing by near-infrared fluorescence imaging shortly after bone marrow transplantation. PLoS One 2010; 5: e11114.
28. Whelan JA, Russell NB, Whelan MA. A method for the absolute quantification of cDNA using real-time PCR. J Immunol Methods 2003; 278: 261–269.
29. Schmittgen TD, Livak KJ. Analyzing real-time PCR data by the comparative C(T) method. Nat Protoc 2008; 3: 1101–1108.
30. Tyas DA, Simpson TI, Carr CB et al. Functional conservation of Pax6 regulatory elements in humans and mice demonstrated with a novel transgenic reporter mouse. BMC Dev Biol 2006; 6: 21.
31. Diaczok D, Romero C, Zunich J, Marshall I, Radovick S. A novel dominant negative mutation of OTX2 associated with combined pituitary hormone deficiency. J Clin Endocrinol Metab 2008; 93: 4351–4359.
32. Chen S, Wang QL, Nie Z et al. Crx, a novel Otx-like paired-homeodomain protein, binds to and transactivates photoreceptor cell-specific genes. Neuron 1997; 19: 1017–1030.
33. Mangan SH, van Campenhout A, Rush C, Golledge J. Osteoprotegerin upregulates endothelial cell adhesion molecule response to tumor necrosis factor-alpha associated with induction of angiopoietin-2. Cardiovasc Res 2007; 76: 494–505.
34. Vossmerbaeumer U, Ohnesorge S, Kuehl S et al. Retinal pigment epithelial phenotype induced in human adipose tissue-derived mesenchymal stromal cells. Cytotherapy 2009; 11: 177–188.
35. Joe AW, Gregory-Evans K. Mesenchymal stem cells and potential applications in treating ocular disease. Curr Eye Res 2010; 35: 941–952.
36. Bexell D, Gunnarsson S, Tormin A et al. Bone marrow multipotent mesenchymal stroma cells act as pericyte-like migratory vehicles in experimental gliomas. Mol Ther 2009; 17: 183–190.
37. Cavarretta IT, Altanerova V, Matuskova M, Kucerova L, Culig Z, Altaner C. Adipose tissue-derived mesenchymal stem cells expressing prodrug-converting enzyme inhibit human prostate tumor growth. Mol Ther 2010; 18: 223–231.
38. Altanerova V, Cihova M, Babic M et al. Human adipose tissue-derived mesenchymal stem cells expressing yeast cytosinedeaminase:uracil phosphoribosyltransferase inhibit intracerebral rat glioblastoma. Int J Cancer 2012; 130: 2455–2463.
39. Castanheira P, Torquetti LT, Magalhas DR, Nehemy MB, Goes AM. DAPI diffusion after intravitreal injection

of mesenchymal stem cells in the injured retina of rats. Cell Transplant 2009; 18: 423–431.
40. Streilein JW, Stein-Streilein J. Does innate immune privilege exist? J Leukoc Biol 2000; 67: 479–487.
41. Yu SH, Jang YJ, Lee ES, Hwang DY, Jeon CJ. Transplantation of adipose derived stromal cells into the developing mouse eye. Acta Histochem Cytochem 2010; 43: 123–130.
42. Lee ES, Yu SH, Jang YJ, Hwang DY, Jeon CJ. Transplantation of bone marrow-derived mesenchymal stem cells into the developing mouse eye. Acta Histochem Cytochem 2011; 44: 213–221.
43. Zhou HS, Liu DP, Liang CC. Challenges and strategies: the immune responses in gene therapy. Med Res Rev 2004; 24: 748–761.
44. Bull ND, Limb GA, Martin KR. Human Muller stem cell (MIO-M1) transplantation in a rat model of glaucoma: survival, differentiation, and integration. Invest Ophthalmol Vis Sci 2008; 49: 3449–3456.
45. Stout JT, Francis PJ. Surgical approaches to gene and stem cell therapy for retinal disease. Hum Gene Ther 2011; 22: 531–535.
46. Wallace VA. Concise review: making a retina–from the building blocks to clinical applications. Stem Cells 2011; 29: 412–417.
47. Lyon CJ, Evans CJ, Bill BR, Otsuka AJ, Aguilera RJ. The *C. elegans* apoptotic nuclease NUC-1 is related in sequence and activity to mammalian DNase II. Gene 2000; 252: 147–154.
48. McIlroy D, Tanaka M, Sakahira H et al. An auxiliary mode of apoptotic DNA fragmentation provided by phagocytes. Genes Dev 2000; 14: 549–558.
49. Krieser RJ, White K. Engulfment mechanism of apoptotic cells. Curr Opin Cell Biol 2002; 14: 734–738.
50. Goichberg P, Kalinkovich A, Borodovsky N et al. cAMP-induced PKCzeta activation increases functional CXCR4 expression on human CD34+ hematopoietic progenitors. Blood 2006; 107: 870–879.
51. Nakashima M, Akamine A. The application of tissue engineering to regeneration of pulp and dentin in endodontics. J Endod 2005; 31: 711–718.
52. Lue Y, Erkkila K, Liu PY et al. Fate of bone marrow stem cells transplanted into the testis: potential implication for men with testicular failure. Am J Pathol 2007; 170: 899–908.
53. Walter M, Liang S, Ghosh S, Hornsby PJ, Li R. Interleukin 6 secreted from adipose stromal cells promotes migration and invasion of breast cancer cells. Oncogene 2009; 28: 2745–2755.
54. Kucerova L, Matuskova M, Hlubinova K, Altanerova V, Altaner C. Tumor cell behaviour modulation by mesenchymal stromal cells. Mol Cancer 2010; 9: 129.
55. Crane IJ, Liversidge J. Mechanisms of leukocyte migration across the blood-retina barrier. Semin Immunopathol 2008; 30: 165–177.
56. Zderic V, Vaezy S, Martin RW, Clark JI. Ocular drug delivery using 20-kHz ultrasound. Ultrasound Med Biol 2002; 28: 823–829.
57. Runkle EA, Antonetti DA. The blood-retinal barrier: structure and functional significance. Methods Mol Biol 2011; 686: 133–148.
58. Haurigot V, Villacampa P, Ribera A et al. Increased intraocular insulin-like growth factor-I triggers blood-retinal barrier breakdown. J Biol Chem 2009; 284: 22961–22969.
59. Frey T, Antonetti DA. Alterations to the blood-retinal barrier in diabetes: cytokines and reactive oxygen species. Antioxid Redox Signal 2011; 15: 1271–1284.
60. Funatsu H, Yamashita H, Nakamura S et al. Vitreous levels of pigment epithelium-derived factor and vascular endothelial growth factor are related to diabetic macular edema. Ophthalmology 2006; 113: 294–301.
61. Funatsu H, Yamashita H, Ikeda T, Mimura T, Eguchi S, Hori S. Vitreous levels of interleukin-6 and vascular endothelial growth factor are related to diabetic macular edema. Ophthalmology 2003; 110: 1690–1696.
62. Funatsu H, Yamashita H, Noma H et al. Aqueous humor levels of cytokines are related to vitreous levels and progression of diabetic retinopathy in diabetic patients. Graefes Arch Clin Exp Ophthalmol 2005; 243: 3–8.
63. Noma H, Funatsu H, Mimura T, Harino S, Hori S. Aqueous humor levels of vasoactive molecules correlate with vitreous levels and macular edema in central retinal vein occlusion. Eur J Ophthalmol 2010; 20: 402–409.
64. Kilroy GE, Foster SJ, Wu X et al. Cytokine profile of human adipose-derived stem cells: expression of angiogenic, hematopoietic, and pro-inflammatory factors. J Cell Physiol 2007; 212: 702–709.
65. Fischer C, Schneider M, Carmeliet P. Principles and therapeutic implications of angiogenesis, vasculogenesis and arteriogenesis. Handb Exp Pharmacol 2006; 176 Pt 2: 157–212.
66. Lange CA, Bainbridge JW. Oxygen sensing in retinal health and disease. Ophthalmologica 2012; 227: 115–131.
67. Kujawa MJ, Carrino DA, Caplan AI. Substrate-bonded hyaluronic acid exhibits a size-dependent stimulation of chondrogenic differentiation of stage 24 limb mesenchymal cells in culture. Dev Biol 1986; 114: 519–528.
68. Li L, Xie T. Stem cell niche: structure and function. Annu Rev Cell Dev Biol 2005; 21: 605–631.
69. Engler AJ, Sen S, Sweeney HL, Discher DE. Matrix elasticity directs stem cell lineage specification. Cell 2006; 126: 677–689.
70. Bagherpoor AJ, Bahrami AR, Matin MM, Mahdavi-Shahri N, Edalatmanesh MA. Investigating the effects of vitreous humour (crude extract) on growth and differentiation of rat mesenchymal stem cells (rMSCs) and human NTERA2 cells. Tsitol Genet 2010; 44: 15–21.
71. Chen XD. Extracellular matrix provides an optimal niche for the maintenance and propagation of mesenchymal stem cells. Birth Defects Res C Embryo Today 2010; 90: 45–54.
72. Baudouin C, Fredj-Reygrobellet D, Brignole F, Negre F, Lapalus P, Gastaud P. Growth factors in vitreous and subretinal fluid cells from patients with proliferative vitreoretinopathy. Ophthalmic Res 1993; 25: 52–59.